

Advancing Welding Defect Detection in Maritime Operations via Adapt-WeldNet and Defect Detection Interpretability Analysis

Kamal Basha S and Athira Nambiar

Department of Computational Intelligence,
Faculty of Engineering and Technology,
SRM Institute of Science and Technology,
Kattankulathur, Tamil Nadu, 603203, India

c58527@srmist.edu.in, athiram@srmist.edu.in

Best Paper Award – Accepted at the International Conference on AI for the Oceans (ICAIO) 2025.

To appear in Springer Lecture Notes in Networks and Systems (LNNS). This is the pre-publication version.

Abstract

Weld defect detection is crucial for ensuring the safety and reliability of piping systems in the oil and gas industry, especially in challenging marine and offshore environments. Traditional non-destructive testing (NDT) methods often fail to detect subtle or internal defects, leading to potential failures and costly downtime. Furthermore, existing neural network-based approaches for defect classification frequently rely on arbitrarily selected pretrained architectures and lack interpretability, raising safety concerns for deployment. To address these challenges, this paper introduces “Adapt-WeldNet”, an adaptive framework for welding defect detection that systematically evaluates various pre-trained architectures, transfer learning strategies, and adaptive optimizers to identify the best-performing model and hyperparameters, optimizing defect detection and providing actionable insights. Additionally, a novel Defect Detection Interpretability Analysis (DDIA) framework is proposed to enhance system transparency. DDIA employs Explainable AI (XAI) techniques, such as Grad-CAM and LIME, alongside domain-specific evaluations validated by certified ASNT NDE Level II professionals. Incorporating a Human-in-the-Loop (HITL) approach and aligning with the principles of Trustworthy AI, DDIA ensures the reliability, fairness, and accountability of the defect detection system, fostering confidence in automated decisions through expert validation. By improving both performance and interpretability, this work enhances trust, safety, and reliability in welding defect detection systems, supporting critical operations in offshore and marine environments.

Keywords: Welding Defect Detection, Explainable AI, Adaptive AI, Adapt-WeldNet, DDIA, Human-in-the-Loop (HITL), Trustworthy AI

1 Introduction

Welding is a fabrication process in which two or more materials, typically metals, are joined together by causing coalescence through the application of heat, pressure, or both. It plays a pivotal role in the construction and maintenance of maritime offshore structures, including oil rigs, pipelines, and support vessels, due to its efficiency and versatility [14]. In offshore applications, precise welding is essential to ensure the structural integrity of components that must withstand harsh marine environments, dynamic loads, and corrosive conditions [18].

Despite its critical importance, welding in maritime offshore structures is susceptible to various defects such as cracks, porosity, and lack of penetration, which can severely compromise safety and performance [25]. Non-Destructive Testing (NDT) techniques [12], including ultrasonic, radiographic, and magnetic particle testing, are essential for identifying these flaws and ensuring compliance with maritime safety standards. However, traditional NDT methods may struggle to detect subtle or internal defects effectively, especially under challenging offshore conditions. In recent years, advanced AI-driven techniques have emerged as transformative tools, offering improved defect detection accuracy, automating inspection processes, and enhancing maintenance strategies, all of which contribute to the reliability and longevity of offshore structures [24]. However, challenges remain in applying these advanced technologies to welding defect detection, particularly in offshore environments where domain-specific issues such as harsh marine conditions complicate matters. Pre-trained models, while effective in some general scenarios, often underperform in these contexts due to a lack of optimization for domain-specific parameters.

To overcome these limitations, we propose a novel framework “**Adapt-WeldNet**”, that adaptively optimizes the model through adaptive transfer Learning, adaptive model selection, and adaptive optimizer and hyperparameters. This approach is specifically designed for welding defect detection in offshore environments. By dynamically selecting the best parameters and model configurations, Adapt-WeldNet aims to deliver the most effective trial for developing a classifier. This ensures improved performance in detecting and addressing welding flaws, tailored to the unique and challenging conditions of offshore structures.

Despite the promising capabilities of AI in defect detection, yet another critical limitation is the lack of interpretability in black-box models. The inability to understand how models arrive at their decisions undermines trust and hinders their adoption, especially in high-stakes applications like welding defect detection in offshore environments. To this end, Explainable AI (XAI) has emerged as an efficient solution towards providing transparency, accountability, and trust in machine learning models by making their decision-making processes more understandable and interpretable to humans. Recent works have proposed various evaluation metrics for XAI methods, including reference-based metrics such

as Pearson correlation coefficient (PCC) and similarity (SIM), which compare explanation maps with human-interpreted maps or pixel importance in input images [5]. The Defense Advanced Research Projects Agency (DARPA) [11] also highlights the importance of XAI in critical applications. In these scenarios, where safety and reliability are paramount, XAI plays a key role in building trust and ensuring the adoption of AI-driven defect detection systems.

In welding defect detection, the application of XAI is still underexplored. In this regard, we propose the **Defect Detection Interpretability Analysis (DDIA) framework**, which incorporates Human-in-the-Loop and Trustworthy AI principles. This framework allows domain experts in welding to provide human interpretations, ensuring the transparency and reliability of AI-driven defect detection. Furthermore, DDIA includes quantitative metrics for interpretability in defect localization, enabling an objective evaluation of defect detection models. As part of this framework, we propose a novel **recall-based evaluation metric** for the interpretability of XAI techniques in defect localization, marking this as the first domain-specific evaluation of XAI in welding defect detection. The key contributions of this paper include:

- A novel ”**Adapt-WeldNet**”, an adaptive AI framework for optimizing the model selection and parameter tuning in welding defect detection.
- The **Defect Detection Interpretability Analysis (DDIA)** framework, a novel approach for evaluating the performance of different XAI methods through domain expert analysis, one of its first kind.
- Proposal of a novel ‘**recall-based evaluation metric**’ for the interpretability of XAI techniques for defect localization.
- Extensive quantitative and qualitative analysis on a real-world welding dataset.

2 Related works

Traditional welding defect detection methods, like visual inspection and NDT, face accuracy limitations. A machine vision algorithm [26] has achieved 95% accuracy, reaching up to 99% in real-world applications. Recent advancements in weld defect detection have explored a variety of deep learning models, including both pre-trained models and novel architectures. [28] presents an ensemble-based deep learning model for welding defect detection and classification, achieving 93.12% accuracy in Non-Destructive Testing (NDT) of submerged arc welds. Pre-trained models such as AlexNet, VGG-16, VGG-19, ResNet50, and GoogLeNet have demonstrated excellent performance, particularly with the application of data augmentation techniques on datasets like GDXray [2]. Fine-tuning strategies using VGG16 and ResNet50 on augmented X-ray datasets have also yielded effective results, with VGG16 achieving 90% accuracy despite data imbalance [16]. In specific applications like TIG welding defect classification, models such as

VGG16, VGG19, ResNet50, InceptionV3, and MobileNetV2 have been successfully applied with various optimizers, achieving high accuracy [22].

Transfer learning has played a key role in improving defect detection across different welding techniques. For instance, transfer learning with GoogLeNet and Multi-Layer Perceptron (MLP) has resulted in a 96.99% classification accuracy for spot-welding evaluations [29]. Moreover, a deep transfer learning model has been successfully applied to aeronautics composite materials, achieving 96% accuracy and demonstrating robustness even with limited labeled data [10].

In addition to traditional models, recent work has explored more advanced architectures like the Vision Transformer (ViT), which has been incorporated into a Deep Feature Extraction Module (DFEM) for enhanced X-ray weld defect detection [32]. Similarly, VAE-DCGAN—a combination of a Variational Autoencoder (VAE) with a Deep Convolutional GAN (DCGAN)—has been employed for improved feature representation in weld joint defects, leading to better defect detection performance [9]. Furthermore, Faster RCNN-based models have also been explored for their potential in real-time weld defect detection applications [1]. Finally, real-time applications, such as WelDeNet, a deep CNN with 14 convolutional layers, have achieved remarkable accuracy (99.5%) in welding defect classification, demonstrating their applicability in practical, time-sensitive environments [19].

In contrast to the aforementioned works, “Adapt-WeldNet” offers an optimal solution by leveraging adaptive transfer learning, adaptive models, and adaptive optimizers. Similarly, the Defect Detection Interpretability Analysis (DDIA) framework goes beyond applying XAI by integrating domain experts into the loop, fostering a trustworthy AI system tailored for the maritime offshore industrial environment.

3 Methodology

In this section, we present the comprehensive methodology adopted in this study. Figure 1 illustrates the architectural workflow of the proposed Adapt-WeldNet framework. Initially, images representing 4 types for images i.e. crack (C), lack of penetration (LP), porosity (P), and no defect are fed into an image preprocessing pipeline. After preprocessing, the Adapt-WeldNet framework optimizes model performance under varying conditions, incorporating adaptive transfer learning, adaptive model selection, and adaptive optimizer and hyperparameter tuning, as discussed in Section 3.1. The best-performing classifier, identified through the Adapt-WeldNet framework, is further developed and evaluated using explainable AI (XAI) techniques, detailed in Section 3.2. Further advancing this, the proposed Defect Detection Interpretability Analysis (DDIA) framework enhances the evaluation of XAI by incorporating assessments from welding experts, thereby improving the interpretability and reliability of the results. The DDIA framework is discussed in detail in Section 3.3. After receiving expert validation, the model is deployed for safe and transparent defect detection.

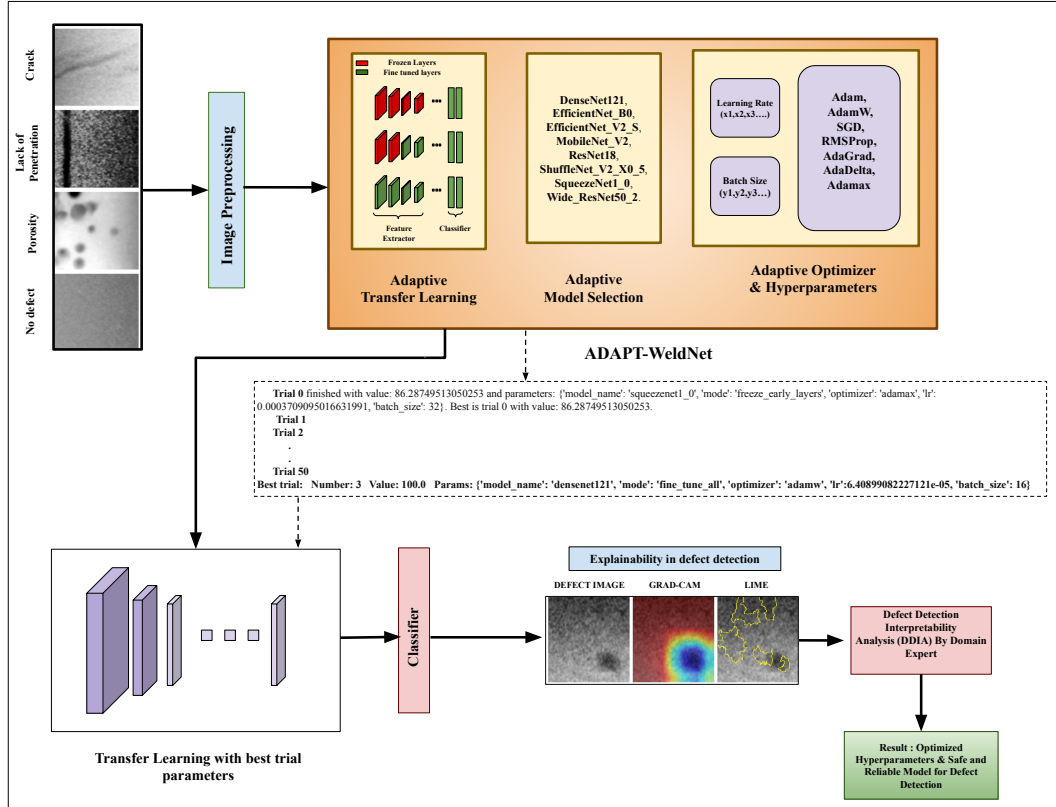


Figure 1: Proposed **Adapt-WeldNet** framework for welding defect detection, integrating adaptive models, adaptive transfer learning, adaptive optimizers, and hyperparameter tuning, alongside the DDIA framework with Explainable AI (XAI) for enhanced interpretability and performance.

3.1 Adapt-WeldNet framework

Most existing works on weld defect detection relies on using random architectures with arbitrary parameters, which may not be well-suited for this critical domain. This lack of systematic optimization can lead to suboptimal results, raising concerns about reliability and trustworthiness during deployment, especially in critical maritime offshore structures. To address this, the Adapt-WeldNet framework is designed to optimize model selection and parameter tuning. By systematically identifying the best-performing architectures and parameters, this approach ensures greater transparency and trustworthy AI, making it more suitable for high-stakes applications.

Initially, the input defect images are fed into a preprocessing pipeline, where operations such as image resizing and normalization are performed. The preprocessed images are then passed to the Adapt-WeldNet framework, which employs

adaptive model selection. This process involves evaluating eight neural network architectures pre-trained on ImageNet, utilizing three adaptive transfer learning strategies. Additionally, the framework explores seven different optimizers, along with varying learning rates and batch sizes, to identify the best model tailored for this specific domain. The optimization process is guided by the Optuna library [3] , and further details are provided below.

- **Adaptive Model Selection:** The model name is chosen from the following options: ResNet18, DenseNet121, EfficientNet-B0, EfficientNet-V2-S, MobileNet-V2, Wide ResNet50-2, ShuffleNet V2 X0.5, and SqueezeNet1.0.
- **Adaptive Transfer Learning:** Transfer learning [30] involves leveraging a pre-trained model on a similar task and adapting it to a new task, often by fine-tuning certain layers. The model training mode is selected from three options:
 - *Freeze Early Layers*: In this mode, the early layers of the pre-trained model are frozen to retain learned features, while the later layers, including the classifier, are fine-tuned to adapt to the new dataset.
 - *Freeze All Layers*: Here, all layers of the pre-trained model except for the final classifier are frozen, and only the classifier is trained to adapt to the new task.
 - *Fine-tune All*: This approach involves fine-tuning all layers of the pre-trained model to fully adapt it to the new dataset.
- **Adaptive Optimizer and Hyperparameters:** The optimizer is chosen from the following options: Adam [15], AdamW [17], SGD[21], RM-Sprop [13], Adagrad [7], Adadelta [31], and Adamax [15]. These optimizers are designed to improve model convergence during training. Additionally, the **learning rate** is optimized from a log-uniform distribution between 1×10^{-5} and 1×10^{-2} and the **batch size** is chosen from the options: 16, 32, and 64.

The Adapt-WeldNet framework systematically selects the optimal combination of parameters through trial and error, ultimately resulting in the best-performing model configuration for weld defect detection. The classifier is developed using the best hyperparameters identified through this process. To further enhance the interpretability and transparency of the model, additional explainable AI (XAI) techniques, such as Grad-CAM and LIME, are applied.

3.2 Explainability Techniques

Grad-CAM and LIME are employed to provide insights into the classifier’s decision-making process, offering a deeper understanding of its predictions. Below are the mathematical formulations and implementation details of these techniques.

3.2.1 Grad-CAM (Gradient-weighted Class Activation Mapping)

Grad-CAM [23] generates a heatmap by computing the weighted sum of the feature maps from the last convolutional layer, where the weights are determined by the gradients of the output class score y^c with respect to these feature maps:

$$L^c = \text{ReLU} \left(\sum_k \left(\frac{1}{Z} \sum_{i,j} \frac{\partial y^c}{\partial A_{ij}^k} \right) A^k \right) \quad (1)$$

In this equation, L^c represents the Grad-CAM heatmap for class c , highlighting the regions of the image that influence the model's prediction for that class. The function ReLU ensures only positive contributions are considered. The term \sum_k denotes the summation over all feature maps k . The weights for each feature map are computed by averaging the gradients of the class score y^c with respect to the feature map activations A_{ij}^k over all spatial locations (i,j) , normalized by the total number of pixels Z in the feature map. Finally, each feature map A^k is weighted by its corresponding importance and summed to produce the heatmap.

3.2.2 LIME (Local Interpretable Model-agnostic Explanations)

LIME [20] explains predictions by perturbing input data and fitting a simple model to the perturbed samples, minimizing the locality-aware loss:

$$L(f_p, g, \pi_x) = \sum_{z \in Z} \pi_x(z) (f_p(z) - g(z))^2 \quad (2)$$

Where $f_p(z)$ is the prediction of the complex model, $g(z)$ is the simpler model, and $\pi_x(z) = \exp\left(-\frac{D(x,z)^2}{\sigma^2}\right)$ gives higher weight to samples close to x , ensuring a local approximation of the complex model.

3.3 Defect Detection Interpretability Analysis (DDIA) Framework with Expert Guided Evaluation

While explainable AI (XAI) plays a pivotal role in making deep learning models interpretable, the Defect Detection Interpretability Analysis (DDIA) framework advances this by incorporating a human-in-the-loop approach, involving certified domain experts. This ensures a comprehensive evaluation of the AI model, addressing not only interpretability but also reliability and alignment with real-world requirements. In particular, the DDIA framework leverages feedback from specialists, such as ASNT NDE Level II [4] auditors, who assess critical factors like detection accuracy, defect visibility, image quality, defect type, and prediction confidence. By analyzing XAI outputs, such as Grad-CAM and LIME explainers, these experts trace the model's decision-making process and identify areas for improvement, such as refining the dataset or retraining the model to enhance robustness.

Defect Detection Interpretability Analysis (DDIA)

1015 files

Image 1 of 1015

Was the defect detected?

Was the defect detected? (Grad-CAM)

Was the defect detected? (LIME)

What is the quality of the image?

What is the quality of the image? (Grad-CAM) Good Noisy Overexposed Underexposed

What is the quality of the image? (LIME) Good Noisy Overexposed Underexposed

How visible is the defect?

How visible is the defect? (Grad-CAM) Clearly Visible Partially Visible Not Visible

How visible is the defect? (LIME) Clearly Visible Partially Visible Not Visible

What type of defect is detected?

What type of defect is detected? (Grad-CAM) Crack Porosity Lack of Fusion Others

What type of defect is detected? (LIME) Crack Porosity Lack of Fusion Others

How confident are you in the explanation (1-5)?

How confident are you in the explanation (1-5)? (Grad-CAM)

How confident are you in the explanation (1-5)? (LIME)

Figure 2: Defect Detection Interpretability Analysis (DDIA) Framework

The DDIA framework as shown in Figure 2 is designed to tackle real-world challenges encountered in X-ray imaging, such as overexposure, underexposure, noise. It incorporates a structured evaluation mechanism, wherein XAI results are presented to experts under various X-ray film scenarios. This mechanism includes targeted questions aimed at assessing: The defect detection is evaluated by determining whether the defect was detected (Yes/No for both Grad-CAM and LIME). The image quality is assessed as clear, underexposed, overexposed, or noisy. Defect visibility is rated as clearly visible, partially visible, or not visible for both Grad-CAM and LIME. The defect type is categorized as crack, lack of penetration (LP), or porosity. Lastly, auditors assign confidence scores ranging from 1 to 5 for both Grad-CAM and LIME explanations.

These structured inputs enable a detailed analysis of the XAI results, categorizing X-ray films by quality (e.g., clear, noisy, overexposed, underexposed)

and identifying the strengths of each explainer. For instance, the analysis reveals which XAI method, Grad-CAM or LIME, provides higher confidence to auditors and performs better under specific conditions.

By integrating domain expertise into the evaluation process, the DDIA framework fosters trust and ensures safer deployment of AI systems in high-stakes environments like offshore marine structures. This human-in-the-loop approach not only enhances model transparency but also addresses critical safety concerns, making it one of the first frameworks to combine XAI and expert audits in welding defect detection for maritime applications.

4 Experimental Setup

In this section, we present the experimental setup, including the dataset described in Section 4.1 and the evaluation metrics outlined in Section 4.2, which are applied to assess the performance of the Adaptive AI model selection and Explainable AI techniques.

4.1 Dataset

The experiments utilized the RIAWELC dataset [27], that consists of 24,407 X-ray weld images categorized into four defect classes: porosity(P), lack of penetration (LP), crack(C), and no defects(ND). For each experiment, the dataset is divided into training and validation sets, ensuring a balanced representation of each class in both sets. Initially, the class distribution in the training dataset was uneven, with 7008 samples for crack, 3712 samples for low penetration, 5352 samples for no defects, and 5768 samples for porosity. After applying data augmentation techniques, the dataset was balanced, resulting in 7008 samples for each class.

4.2 Evaluation Metrics

4.2.1 Accuracy and Confusion Matrix

Accuracy measures the proportion of correctly classified instances, calculated as the ratio of true positives (TP) and true negatives (TN) to the total instances, including false positives (FP) and false negatives (FN). A confusion matrix provides a detailed breakdown of the classification performance by showing TP, TN, FP, and FN, helping to understand the model's errors and successes [6, 8].

4.2.2 Quantitative Metrics for Interpretability in Defect Localization

To assess the interpretability of Grad-CAM in localizing welding defects, we employ a novel recall-based evaluation method. This quantitative metric measures the ability of Grad-CAM to correctly identify defect regions in welding images. The dataset used for this evaluation comprises 1,031 annotated images, including defects such as cracks, porosity, and lack of penetration (LP), with annotations provided by certified domain experts.

Recall, a key metric for this analysis, is defined as:

$$\text{Recall} = \frac{\sum_i (L_i^c \cdot G_i)}{\sum_i G_i} \quad (3)$$

Here, L_i^c represents the Grad-CAM heatmap for the i -th image and class c , while G_i denotes the ground truth defect region for the i -th image. This formulation ensures that the overlap between Grad-CAM predictions and expert-annotated ground truth regions is accurately measured.

To evaluate overall performance, we compute the Average Recall, defined as the mean of recall values across all images in the dataset:

$$\text{Average Recall} = \frac{1}{N} \sum_{i=1}^N \frac{\sum(L_i^c \cdot G_i)}{\sum G_i} \quad (4)$$

Where N represents the total number of images. This metric provides a comprehensive evaluation of Grad-CAM’s ability to localize defect regions across a diverse dataset.

Recall measures how much of the defect area the model was able to detect. A recall of 1 (or 100%) means the model found all the defect pixels in the ground truth. A recall of 0.5 means the model detected only half of the defect pixels. This shows how well Grad-CAM identifies defect regions, with varying recall values reflecting the model’s performance across different defects and image conditions.

4.3 Implementation details

The training procedure involved selecting various models such as DenseNet121, EfficientNet-B0, MobileNet-V2, ResNet18, ShuffleNet-V2 x0.5, SqueezeNet1.0, and WideResNet50-2, each initialized with pre-trained ImageNet weights. The final fully connected layer was adjusted to match the output classes of the dataset. Three training modes were employed: Freeze All Layers (where all layers are frozen and only the classifier head is trained), Freeze Early Layers (where the early layers are frozen and only the deeper layers and classifier head are trained), and Fine-Tuning All Layers (where all model parameters are updated).

For model optimization, we utilized the Adapt-Weld framework to tune hyperparameters, including model architecture, optimizer type, learning rate, and batch size. The function `train_and_evaluate` handles the training and evaluation process. The model, training mode, and dataset are specified, and the Cross-Entropy Loss is used as the loss function. The selected optimizer is applied during training, and early stopping is employed with a patience value to prevent overfitting.

The `objective` function defines the search space for Optuna, allowing it to suggest the best model architecture, optimizer type, learning rate, and batch size. Specifically, the model architecture (e.g., ResNet18, DenseNet121, EfficientNet-B0, etc.) will be selected from Adapt-Weld framework, the training mode (Freeze All Layers, Freeze Early Layers, or Fine-Tuning All Layers), the optimizer type (Adam, AdamW, SGD, RMSProp, AdaGrad, AdaDelta, or Adamax), the learning rate (ranging from 1e-5 to 1e-2), and the batch size (16, 32, or 64).

The model is loaded according to the trial’s suggestions, and the corresponding training configuration is applied. The training loop runs for 100 epochs, with

early stopping if the validation accuracy does not improve for five consecutive epochs. After each epoch, the model’s performance is evaluated on the validation set.

5 Experimental Results

The experimental results of our proposed Adapt-WeldNet framework is presented in this section. We first discuss the quantitative results in Section 5.1, followed by qualitative results of Explainable AI (XAI) in Section 5.2. Section 5.3 covers the quantitative analysis of the Defect Detection Interpretability Analysis (DDIA) framework. Lastly, we provide the quantitative metrics for interpretability in defect localization in Section 5.4.

5.1 Quantitative Results of ADAPT-WeldNet

5.1.1 Adapt-WeldNet Optimization Results:

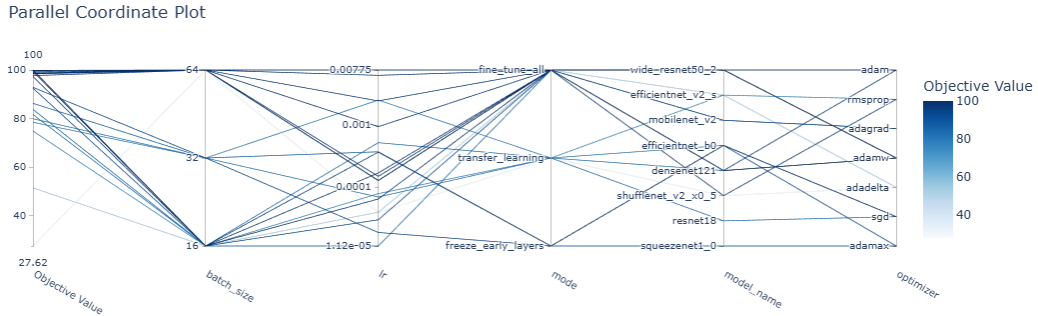


Figure 3: Parallel coordinate plot showing the relationship between hyperparameters and the objective value in the adaptive AI model optimization process. Darker colors indicate higher objective values.(Best viewed in colour)

The parallel coordinate plot in Figure 3 illustrates the impact of various hyperparameters, including batch size, learning rate, mode, model architecture, and optimizer, on the objective value during the optimization of the adaptive AI model for welding defect detection. The results demonstrate that fine-tuning all layers consistently achieves superior performance compared to freezing early layers. Models such as *EfficientNet_B0*, *EfficientNet_V2_S*, and *DenseNet121* exhibit the best performance when combined with optimizers like AdamW or Adam at lower learning rates (e.g., 1×10^{-5}). Additionally, extreme batch sizes—both small (16) and large (64)—are associated with higher objective values, while medium batch sizes (32) show more variability. These findings underscore the significance of hyperparameter tuning and adaptive AI techniques in optimizing model performance for specific domains like welding defect detection.

Figure 4 shows the Adapt-Weld framework optimization results for hyperparameter tuning across various configurations, including batch size, learning

rate (lr), training mode, model architectures, and optimizers. The objective value represents the validation accuracy achieved for each trial, with the color intensity indicating the trial number.

Models with a batch size of 16 generally achieved higher objective values compared to larger batch sizes (32 and 64). Learning rates in the range of 10^{-5} to 10^{-3} showed consistent performance, with a few trials achieving near-optimal objective values. The fine-tune-all mode outperformed the other modes (transfer learning and freezing early layers), highlighting the benefit of updating all layers during training. DenseNet121 and WideResNet50-2 consistently showed superior objective values compared to other models such as MobileNet-V2 and ShuffleNet-V2 x0.5. Among the optimizers, Adam and AdamW showed the best performance, whereas SGD and RMSprop exhibited slightly lower objective values in most trials.

These results emphasize the importance of hyperparameter tuning to achieve optimal performance and reveal the sensitivity of performance to specific configurations.

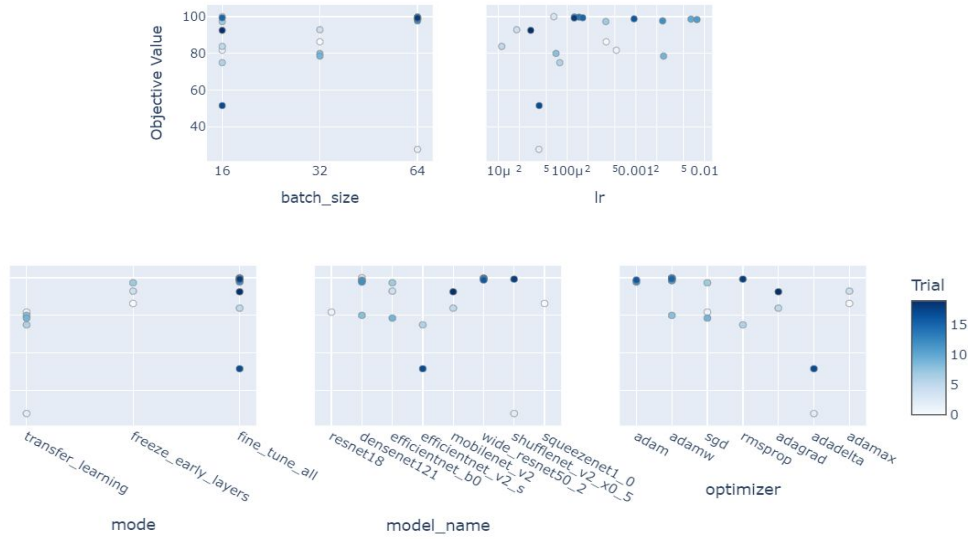


Figure 4: Hyperparameter tuning results of Adapt-WeldNet for batch size, learning rate, training mode, model architecture, and optimizer.

5.1.2 Effect of Parameter Tuning Modes:

Figure 5 presents the comparative performance of three parameter tuning modes: *transfer learning*, *freeze_early_layers*, and *fine_tune_all*. The box plot highlights that fine-tuning all layers achieves the highest performance consistency, with minimal variation and only a few outliers. Freezing early layers also maintains robust performance, whereas transfer learning in freezing all layers shows comparatively lower values and larger variability.

5.1.3 Classifier Performance Evaluation from Best Hyperparameters:

The classifier, optimized using the best parameters identified by Adapt-Weld, was evaluated for its performance on the welding defect detection task. The model architecture selected is DenseNet121, fine-tuned in the "fine-tune all" mode, where all layers were updated during training. The optimizer used is AdamW with a learning rate of 6.41×10^{-5} , chosen to ensure efficient convergence. A batch size of 16 was used for training to balance memory usage and model performance. The confusion matrix, presented in Figure 6, provides insights into the model's classification accuracy across the four defect categories: porosity (P), lack of penetration (LP), crack (C), and no defects.

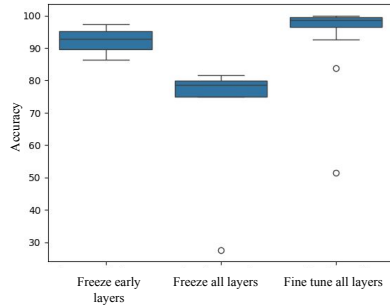


Figure 5: Comparison of Adaptive Transfer learning: freezing early layers, Freeze all layers, and fine-tuning all layers.

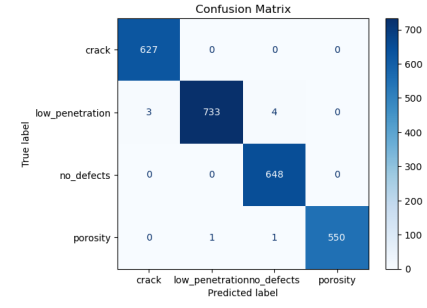


Figure 6: Confusion matrix of the classifier, showcasing its performance across the four defect categories.

5.2 Qualitative XAI Results

The explainability analysis of welding defect detection using Grad-CAM and LIME demonstrates their effectiveness under different imaging conditions as represented in Figure 7. It is observed that Grad-CAM provides a broad visualization of defect regions, highlighting the areas of interest across defect categories such as *Crack*, *Lack of Penetration (LP)*, and *Porosity (P)*. The method effectively adapts to varying conditions, including clear, overexposed, underexposed, and noisy images. Whereas LIME complements Grad-CAM by offering localized, boundary-focused explanations. It highlights fine-grained regions, aiding in the detailed interpretation of the model's predictions. Grad-CAM is particularly reliable for identifying larger and more prominent defect regions, whereas LIME excels at pinpointing smaller, localized areas. However, under challenging conditions like noise and underexposure, Grad-CAM maintains robust defect localization, while LIME exhibits less consistent coverage but retains its ability to focus on specific regions.

Overall, the combination of these methods provides a comprehensive understanding of the model's decision-making process, ensuring reliable detection of

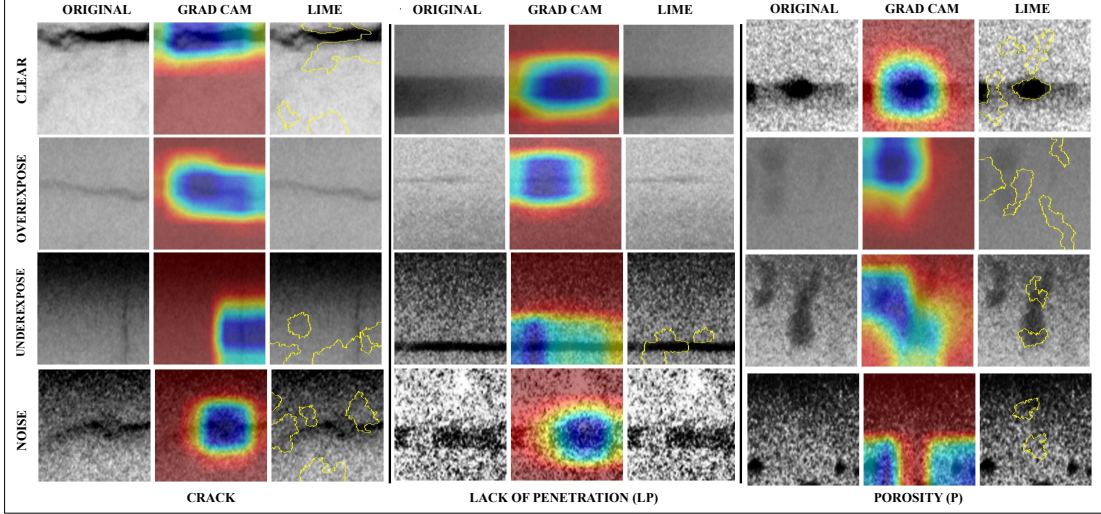


Figure 7: Explainability Analysis of Welding Defect Detection Using XAI Methods

welding defects even under challenging imaging scenarios.

5.3 Quantitative Results of DDIA Framework Analysis

The DDIA framework incorporates a **human-in-the-loop approach**, bridging the gap between domain expertise and AI applications to ensure safe deployment in maritime offshore structures. The comparative analysis in Figure 8 demonstrates: (a) **Impact of Image Quality on XAI Test Set Assessment**, where domain experts assess X-ray films categorized into noisy (14.7%), overexposed (21.7%), underexposed (26.3%), and good quality films (37.3%) to ensure that all critical scenarios are considered, enhancing the robustness of the evaluation; (b) **Defect Detection by Grad-CAM and LIME**, revealing that Grad-CAM provides clearer defect detection with fewer mis detections compared to LIME, making it a more reliable tool for identifying defects; and (c) **Confidence Distribution of XAI Among Domain Experts**, where confidence levels range from 1 (poor) to 5 (excellent). The distribution shows that Grad-CAM receives higher confidence scores, indicating that auditors find it more convincing and easier to use, while LIME scores slightly lower. This analysis highlights which XAI tool domain experts prefer and trust, reinforcing the framework's applicability in critical safety domains. Industrial experts can propose additional XAI techniques based on their specific needs, which will be evaluated according to company guidelines. This continuous feedback loop ensures the DDIA framework remains adaptable and incorporates cutting-edge XAI technologies,

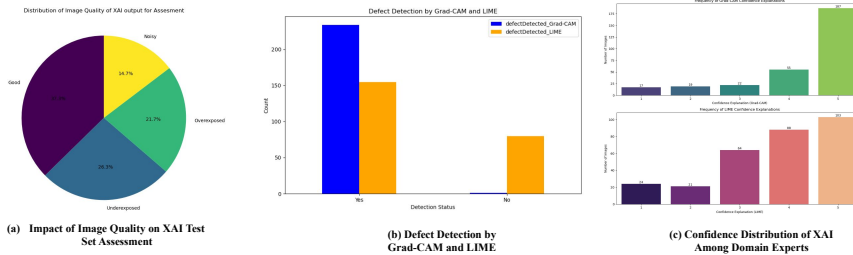


Figure 8: Comparative analysis of Grad-CAM and LIME results: (a) Image Quality on XAI test set, (b) Defect Detection, and (c) Confidence of Domain Experts in XAI tool.

5.4 Quantitative Metrics for Interpretability in Defect Localization

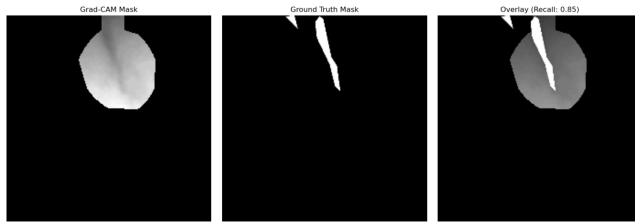


Figure 9: Recall-based evaluation showcasing the Grad-CAM mask, ground truth mask, and recall output for a sample image.

To assess the interpretability and localization performance of Grad-CAM in identifying welding defects, we employed quantitative metrics based on recall. These metrics evaluate the overlap between the predicted defect regions (generated by Grad-CAM) and the ground truth annotations provided by domain experts. By quantifying this overlap, we aim to understand how effectively Grad-CAM highlights the defect regions in welding images.

An example of this evaluation is presented in Figure 9, that visualizes the Grad-CAM mask, the ground truth mask, and the resulting recall output for a sample image. This analysis provides insights into the interpretability of Grad-CAM's predictions and its ability to focus on relevant defect regions. The average recall, calculated across the entire dataset, serves as a comprehensive metric to gauge the model's performance in defect localization:

$$\text{Average Recall} = 0.7722$$

This value highlights the ability of Grad-CAM to consistently localize defect regions, reinforcing its suitability as an XAI tool for welding defect analysis in safety-critical environments.

Acknowledgment

This work received the **Best Paper Award** at the International Conference on AI for the Oceans (ICAIO) 2025. The final version will be published in the *Springer Lecture Notes in Networks and Systems (LNNS)*.

6 Conclusion

This paper presents a framework for welding defect detection in offshore environments using adaptive AI models and Explainable AI (XAI). We introduce a novel framework "Adapt-WeldNet" that combines multiple pre-trained neural networks, optimizes hyperparameters and explores various training modes of transfer learning. XAI techniques, including Grad-CAM and LIME, enhance interpretability and transparency, which are crucial for high-risk applications like welding inspection. Additionally, we introduce the Defect Detection Interpretability Analysis (DDIA) framework, enabling direct interaction between AI models and domain experts, integrating a Human-in-the-loop approach to validate predictions and ensure safety. This DDIA framework supports Trustworthy AI in offshore structures by fostering transparency and accountability. A novel 'recall-based evaluation metric' is also proposed for the interpretability of XAI techniques for defect localization. Our results demonstrate the effectiveness of integrating adaptive AI with XAI to improve both accuracy and interpretability. This study provides a strong foundation for developing reliable, interpretable AI models for defect detection, enhancing operational efficiency, safety, and transparency in industrial environments. Future work will explore advanced XAI methods and extend the approach to other industrial sectors.

References

- [1] Chiraz Ajmi, Juan Zapata, Sabra Elferchichi, and Kaouther Laabidi. Advanced faster-rcnn model for automated recognition and detection of weld defects on limited x-ray image dataset. *Journal of Nondestructive Evaluation*, 43(1):14, 2024. 4
- [2] Chiraz Ajmi, Juan Zapata, Sabra Elferchichi, Abderrahmen Zaafouri, and Kaouther Laabidi. Deep learning technology for weld defects classification based on transfer learning and activation features. *Advances in Materials Science and Engineering*, 2020(1):1574350, 2020. 3
- [3] Takuya Akiba, Shotaro Sano, Toshihiko Yanase, Takeru Ohta, and Masanori Koyama. Optuna: A next-generation hyperparameter optimization framework. In *Proceedings of the 25th ACM SIGKDD international conference on knowledge discovery & data mining*, pages 2623–2631, 2019.

[4] American Society for Nondestructive Testing. American society for non-destructive testing. <https://www.asnt.org/>. Accessed: YYYY-MM-DD. 7

[5] Luca Bourroux, Jenny Benois-Pineau, Romain Bourqui, and Romain Giot. Multi Layered Feature Explanation Method for Convolutional Neural Networks *. In *International Conference on Pattern Recognition and Artificial Intelligence (ICPRAI)*, Paris, France, June 2022. 3

[6] Pedro Domingos. A few useful things to know about machine learning. *Communications of the ACM*, 55(10):78–87, 2012. 9

[7] John Duchi, Elad Hazan, and Yoram Singer. Adaptive subgradient methods for online learning and stochastic optimization. *Journal of machine learning research*, 12(7), 2011. 6

[8] Tom Fawcett. An introduction to roc analysis. *Pattern recognition letters*, 27(8):861–874, 2006. 9

[9] Chen Geng, Sheng Buyun, Fu Gaocai, Chen Xiangxiang, and Zhao Guangde. A gan-based method for diagnosing bodywork spot welding defects in response to small sample condition. *Applied Soft Computing*, 157:111544, 2024. 4

[10] Yanfeng Gong, Hongliang Shao, Jun Luo, and Zhixue Li. A deep transfer learning model for inclusion defect detection of aeronautics composite materials. *Composite structures*, 252:112681, 2020. 4

[11] David Gunning and David W. Aha. Darpa’s explainable artificial intelligence program. *AI Magazine*, 40(2):44–58, 2019. 3

[12] Mridul Gupta, Muhsin Ahmad Khan, Ravi Butola, and Ranganath M Singari. Advances in applications of non-destructive testing (ndt): A review. *Advances in Materials and Processing Technologies*, 8(2):2286–2307, 2022. 2

[13] G. Hinton. Lecture 6c: Neural networks, part 3 (adaptive learning rates). 2012. Lecture notes from the Coursera course on Neural Networks for Machine Learning. 6

[14] Larry F Jeffus, Harold V Johnson, and Al Lesnewich. *Welding: principles and applications*. Delmar Publishers New York, 1999. 2

[15] Diederik P Kingma. Adam: A method for stochastic optimization. *arXiv preprint arXiv:1412.6980*, 2014. 6

[16] Dheeraj Dhruva Kumar, Cheng Fang, Yue Zheng, and Yuqing Gao. Semi-supervised transfer learning-based automatic weld defect detection and visual inspection. *Engineering Structures*, 292:116580, 2023. 3

- [17] I. Loshchilov and F. Hutter. Decoupled weight decay regularization. In *International Conference on Learning Representations (ICLR)*, 2018. 6
- [18] Juan J Manzano-Ruiz and Jose G Carballo. *Multiphase Transport of Hydrocarbons in Pipes*. John Wiley & Sons, 2024. 2
- [19] Stefania Perri, Fanny Spagnolo, Fabio Frustaci, and Pasquale Corsonello. Welding defects classification through a convolutional neural network. *Manufacturing Letters*, 35:29–32, 2023. 4
- [20] Marco Tilio Ribeiro, Sameer Singh, and Carlos Guestrin. ”why should i trust you?”: Explaining the predictions of any classifier, 2016. 7
- [21] H. Robbins and S. Monro. A stochastic approximation method. *The Annals of Mathematical Statistics*, 22(3):400–407, 1951. 6
- [22] Ravi Sekhar, Deepak Sharma, and Pritesh Shah. Intelligent classification of tungsten inert gas welding defects: A transfer learning approach. *Frontiers in Mechanical Engineering*, 8:824038, 2022. 4
- [23] Ramprasaath R. Selvaraju, Michael Cogswell, Abhishek Das, Ramakrishna Vedantam, Devi Parikh, and Dhruv Batra. Grad-cam: Visual explanations from deep networks via gradient-based localization. In *Proceedings of the IEEE International Conference on Computer Vision (ICCV)*, Oct 2017. 7
- [24] Wesley Silva, Ricardo Lopes, Uwe Zscherpel, Dietmar Meinel, and Uwe Ewert. X-ray imaging techniques for inspection of composite pipelines. *Micron*, 145:103033, 2021. 2
- [25] Norsok Standard et al. Welding and inspection of piping. *Standards Norway, Lysaker*, 2004. 2
- [26] Jun Sun, Chao Li, Xiao-Jun Wu, Vasile Palade, and Wei Fang. An effective method of weld defect detection and classification based on machine vision. *IEEE Transactions on Industrial Informatics*, 15(12):6322–6333, 2019. 3
- [27] Benito Totino, Fanny Spagnolo, and Stefania Perri. Riawelc: a novel dataset of radiographic images for automatic weld defects classification. *International Journal of Electrical and Computer Engineering Research*, 3(1):13–17, 2023. 9
- [28] Vinod Vasan, Naveen Venkatesh Sridharan, Rebecca Jeyavadhanam Balasundaram, and Sugumaran Vaithianathan. Ensemble-based deep learning model for welding defect detection and classification. *Engineering Applications of Artificial Intelligence*, 136:108961, 2024. 3
- [29] Ye Yang, Peng Zheng, Hao He, Tianyu Zheng, Lei Wang, and Shan He. An evaluation method of acceptable and failed spot welding products based on image classification with transfer learning technique. In *Proceedings of the 2nd International Conference on Computer Science and Application Engineering*, pages 1–6, 2018. 4

- [30] Jason Yosinski, Jeff Clune, Yoshua Bengio, and Hod Lipson. How transferable are features in deep neural networks? In *Advances in neural information processing systems*, volume 27, 2014. 6
- [31] M.D. Zeiler. Adadelta: An adaptive learning rate method. In *Proceedings of the 30th International Conference on Machine Learning (ICML)*, 2012. 6
- [32] Rui Zhang, Donghao Liu, Qiaofeng Bai, Liuhu Fu, Jing Hu, and Jinlong Song. Research on x-ray weld seam defect detection and size measurement method based on neural network self-optimization. *Engineering Applications of Artificial Intelligence*, 133:108045, 2024. 4